International Journal of Chemical Science
www.chemicaljournals.com
Online ISSN: 2523-2843, Print ISSN: 2523-6075
Received: 28-01-2023, Accepted: 13-02-2023, Published: 02-03-2023
Volume 7, Issue 1, 2023, Page No. 10-14

Efficient removal of highly toxic Cr(VI) from aqueous solution using $FeSb_2$ particles

Sunidhi[1], Manish Srivastava[2], Deepak Gujjar[3*]
[1] Department of Chemistry, Banasthali Vidyapith, Tonk, Rajasthan, India
[2] Department of Chemistry, Allahabad University, Prayagraj, Uttar Pradesh, India
[3] Department of Chemistry, Indian Institute of Technology Roorkee, Roorkee, Uttarakhand, India

Abstract

The unique electronic and crystal structure of intermetallic compounds allows their use for heavy metal removal. Here, we report the synthesis of $FeSb_2$ particles via a green and cost-effective co-precipitation method and their utilization for the efficient removal of highly toxic hexavalent chromium from aqueous solutions. The structure and morphology of $FeSb_2$ particles were confirmed by X-ray diffraction (XRD) and scanning electron microscope (SEM), respectively. Batch adsorption experiments were carried out in Cr (VI) solutions of various concentrations (2-10 mg L^{-1}). Cr (VI) removal by $FeSb_2$ particles was found to follow pseudo-second-order kinetic and Langmuir isotherm models with a maximum adsorption capacity (qm) of 7.79 mg g^{-1}. This study paves the way for other intermetallic compounds for various other wastewater treatments.

Keywords: intermetallics, $FeSb_2$, Co-precipitation method, adsorption, Cr (VI) removal

Introduction

Today's era of urban development and industrial revolution triggers the contamination of water used in daily life as various industries release heavy metals (such as Cr, Pb, As, Hg, Ni, and Ag) as pollutants [1, 2]. Well developed industries such as cement, paper, pigment, leather tanning, and paint use large amount of chromium compounds in various forms such as chromic acid, chromium trioxide, chrome sulfate, etc. for various processes [3, 5] and result in release of noxious Cr(VI) into the various water bodies at a very high concentration (0.5-270 mg L-1) compared to the World Health Organization (WHO) recommended level of 0.05 mg L-1 [6]. The high solubility of Cr(VI) in water allows its contamination to spread very quickly which adversely affects both human and environmental health. Therefore, the removal of toxic Cr(VI) is necessary to keep the clean water supply in balance.

Various methods such as chemical precipitation, ion exchange, membrane filtration, reverse osmosis, bio-adsorption, adsorption, etc. have been employed for many wastewater treatments [7, 11]. But the simplicity, cost-effectiveness and vast applicability of the adsorption process make it more suitable for heavy metal removal [8-11].

Vast literature is available for the adsorptive removal of Cr(VI) using transition metal oxides such as Fe/Mn binary oxide [12], Fe3O4 nanoparticles, [13] Ferrihydroxide/oxohydroxides, [14] and Fe@Fe2O3 core-shell nanowires, [2] but the intermetallics are still untouched in this direction although they exhibit promising properties of high structural, thermal and mechanical stability, and vast range of applications in various fields such as hydrogen storage, thermoelectrics, spintronics, shape memory effect, superconductivity, etc.

In this contribution, we report the successful synthesis of FeSb2 particles via a green co-precipitation method and their utilization for the efficient adsorptive removal of highly toxic Cr(VI) from the aqueous solution.

Material and methods

Chemicals

Anhydrous FeCl3 (Loba Chemie, 99%) and SbCl3 (Alfa Aesar, 99+ %), NaOH pellets (Sigma Aldrich, 97+%), were used as metal precursors and precipitating agent, respectively. Polyvinylpyrrolidone (PVP, Sisco Research Laboratories Pvt. Ltd.) was used as capping agent. K2Cr2O7 (Thermo Fisher Scientific, 99+ %) was used to prepare the Cr(VI) solutions of different concentrations. All the solutions were prepared in distilled water.

FeSb2 synthesis

FeSb2 powder was synthesized via a green co-precipitation approach. First, PVP solution was prepared by dissolving 30 mg PVP (K-30) in the distilled water and placed on a magnetic stirrer. Metal chlorides FeCl3 and SbCl3 in the stoichiometric ratio of 1:2 were dispersed in distilled water via sonication and then, added dropwise into the PVP solution with constant stirring. Thereafter, NaOH solution was injected into the mixture to obtain a precipitate. The precipitates were filtered, dried and transferred to a tube furnace in H2 atmosphere at 650 °C temperature to obtain brownish black FeSb2 powder.

Characterization

The structural phase investigation of as-synthesized FeSb2 sample was carried out using X-ray diffraction (Bruker D8 Advance,) equipped with LINEYE XE detector and CuKα (λ=0.154056 nm) as X-ray source with a step size of 0.02°/s in the continuous scan mode. Microstructural and morphological characteristics were studied using Carl Ziess ultra plus scanning electron microscope (SEM). The residual concentration of Cr(VI) solutions were determined using 4210 Aligents microwave plasma-atomic emission spectrometer (MP-AES).

Adsorption experiment

A stock solution of Cr (VI) of 100 mg L-1 was prepared by dissolving 0.1414 g K2Cr2O7 in 500 mL distilled water, which was further diluted to get Cr(VI) solutions of different concentrations (2-10 mg L-1). Batch adsoprtion experiments were performed by adding 0.02 g of FeSb2 into 50 mL of Cr (VI) solutions of different concentrations at natural pH with constant stirring of 200 rpm for 5 h. A 3 mL of the Cr(VI) solutions were taken out after each pre-determined time interval, filtered and residual Cr(VI) concentrations were determined using MPAES.

The adsorption capacities (in mg g-1) of FeSb2 particles were calculated using mass balance relationship

$$q_t = \frac{(C_0 - C_t)\,V}{m} \qquad (1)$$

Where Co (mg L-1) is the initial Cr(VI) concentration, Ct is the residual concentration of Cr(VI) in mg L-1 at time t, V is the volume (L) of Cr(VI) solution, and m (g) is the amount of FeSb2 used for adsorption. The equilibrium adsorption capacities (qe) was calculated using equation 1 by replacing Ct with Ce (i.e data obtained at 5 h (equilibrium time). The removal percentage of Cr(VI) was calculated using equation 2;

$$\%\,Adsorption = \left(\frac{C_o - C_t}{C_o}\right) \times 100 \qquad (2)$$

The adsorption data were fitted with Lagergren's first order kinetic model (linear form) and Ho's second order kinetic model given below in equations 3 & 4, respectively and two well established models, Langmuir and Freundlich provided in equations 5 & 6, respectively, were applied to understand the interactive mechanism.

$$\ln(q_e - q_t) = \ln(q_e) - k_1 t \qquad (3)$$

$$\frac{t}{q_t} = \frac{1}{k_2 q_e^2} + \frac{t}{q_e} \qquad (4)$$

$$\frac{C_e}{q_e} = \left(\frac{1}{k_L q_m}\right) + \frac{C_e}{q_m} \qquad (5)$$

$$nq_e = lnk_F + \frac{1}{n}\ln C_e \qquad (6)$$

Where Ce, qe, qt, and qm are the equilibrium Cr(VI) concentration (mg L-1), equilibrium adsorption capacity (mg g-1), adsorption capacity (mg g-1) at t time (min), and maximum adsorption capacity (mg g -1), respectively. k1 (min-1), k2 (g mg-1 min-1), KL (L mg-1), and KF, represents the first-order rate constant, second-order rate constant, Langmuir isotherm constant, and Freundlich isotherm constant, respectively.

Result and discussion

Structural analysis

The XRD pattern of as-synthesized FeSb2 particles was recorded in the 2θ range of 20°–90° at room temperature. The pattern shown in Fig. 1a indicates the crystallization of FeSb2 in orthorhombic marcasite phase in Pnnm space group. The relative peak intensities and peak positions of generated pattern are consistent with the referenced XRD pattern (ICCD No: 04-010-4959). The strong reflection peaks correspond to (011), (101), (120), (210), (111), (130), (211) and (031) planes.

The sharp peaks without any significant broadening showed the highly crystalline nature of the particles. The greater intensity of peak at around 31° compared to reference pattern, indicates the preferred orientation along the (011) plane. The SEM images shown in Fig. 1b &1c, suggests the formation of agglomerated particles of non-uniform shape and size in the range of 200-500 nm. The size of particles can be justified based on the high temperature treatment which helps in the particle growth.

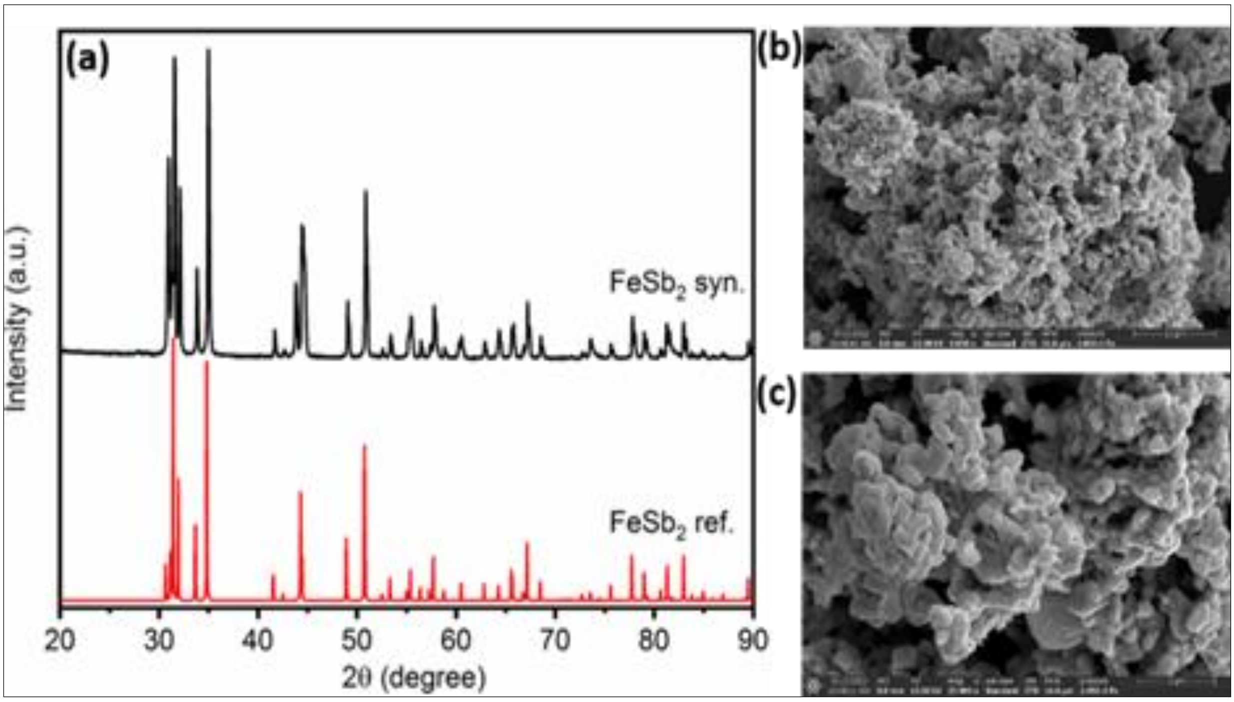

Fig 1: XRD pattern of as-synthesized FeSb$_2$ along with reference data (a), and corresponding SEM images (b & c).

Cr(VI) removal

Batch adsorption experiments were performed at four different Cr(VI) concentrations of 2, 5, 7, and 10 mg L-1 with 0.4 g L-1 FeSb2 dosage and the results are displayed in Fig. 2. The obtained results clearly suggests the fast adsorption rate at the initial stage of contact as about 40 % of Cr(VI) of 2 mg L¬1 was removed within 5 min. The initial fast removal is due to availability of more number of vacant active sites on the FeSb2 surface. Fig. 2a clearly indicate the decrease in removal efficiency of FeSb2 particles with increase in the concentration of Cr(VI) ions. The removal percentage reduced from 94 to 29 % within 120 min on five fold increase in Cr(VI) concentration. This is probably due to increase in competition between Cr(VI) ions for limited number of vacant active sites. On the contrary, the adsorption capacities or net uptake amount of FeSb2 increases from 4.7 to 7.21 mg g-1 on increasing Cr(VI) amount from 2 to 10 mg L-1. The finding is due to enhancement of driving force for external mass transfer on increase in Cr(VI) amount. Also, this can be justified based on the mass-balance relationship (eqn 1) where Co (initial concentration) is present in the numerator part. The experimental data were fitted with two well-known kinetic models: pseudo-first-order and pseudo-second-order as given in Fig. 3. Based on R2 values (Table 1), adsorption of Cr(VI) onto FeSb2 was found to follow pseudo-second-order kinetics. These results suggests the involvement of chemical interaction between Cr(VI) ions and FeSb2 particles and hence, chemisorption as rate controlling step. [15, 16]. The related paramters for both the models are provided in Table 1.

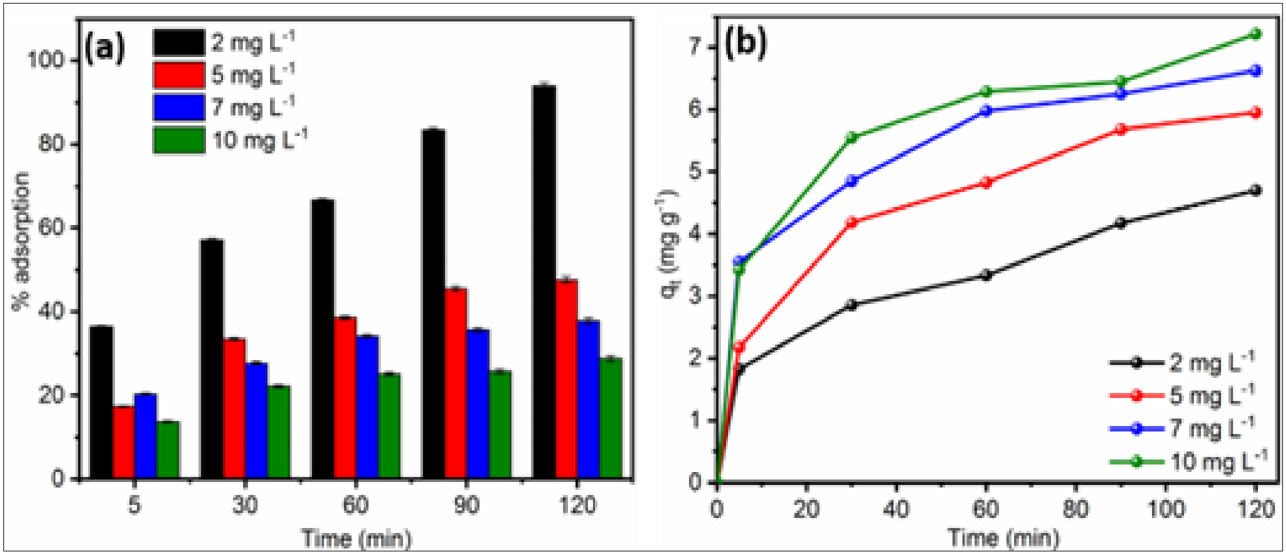

Fig 2: Removal efficiency (a) & adsorption capacity (b) of $FeSb_2$ for the adsorption of Cr(VI) at natural pH and room temperature.

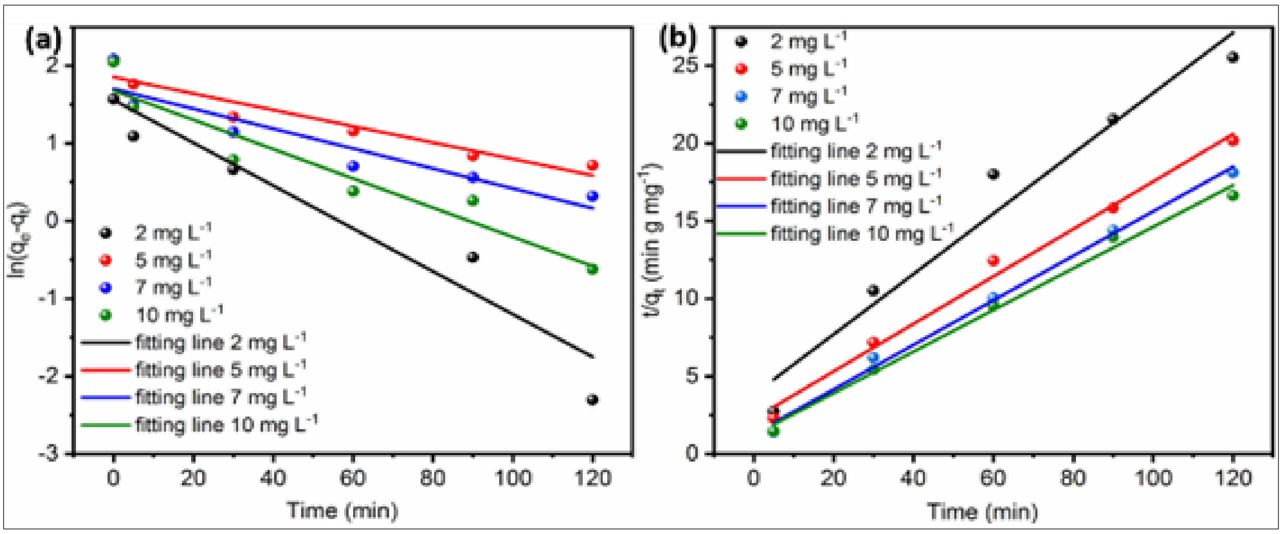

Fig 3: Kinetic models: pseudo-first-order (a) & pseudo-second-order (b) for the removal of Cr(VI) onto $FeSb_2$.

To understand the reaction mechanism, the obtained data were evaluated with Langmuir and Freundlich isotherm models as provided in Fig. 4. The correlation coefficient R2 values (Table 2) strongly indicate the monolayer adsorption of chromium ions on a uniform FeSb2 surface having fixed number of vacant active sites [17] as it follows Langmuir adsorption isotherm. The associated paramters for both isotherm models are provided in Table 2. The maximum adsorption capacity (qm¬) value of 7.79 mg g¬-1 calcualted from Langmuir adsorption isotherm is in good agreement with experimentally achieved maximum equilibrium capacity value of 7.75 mg g-1 (Fig. 5). These results confirm the applicability of Langmuir model for the removal of hexavalent chromium.

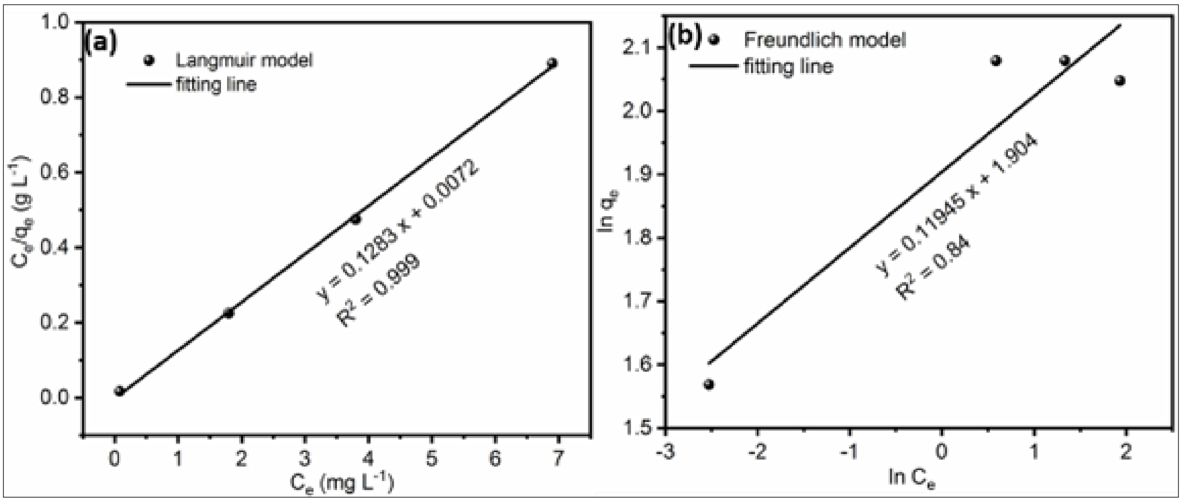

Fig 4: Adsorption isotherms: Langmuir (a) & Freundlich (b) for the removal of Cr(VI) onto $FeSb_2$.

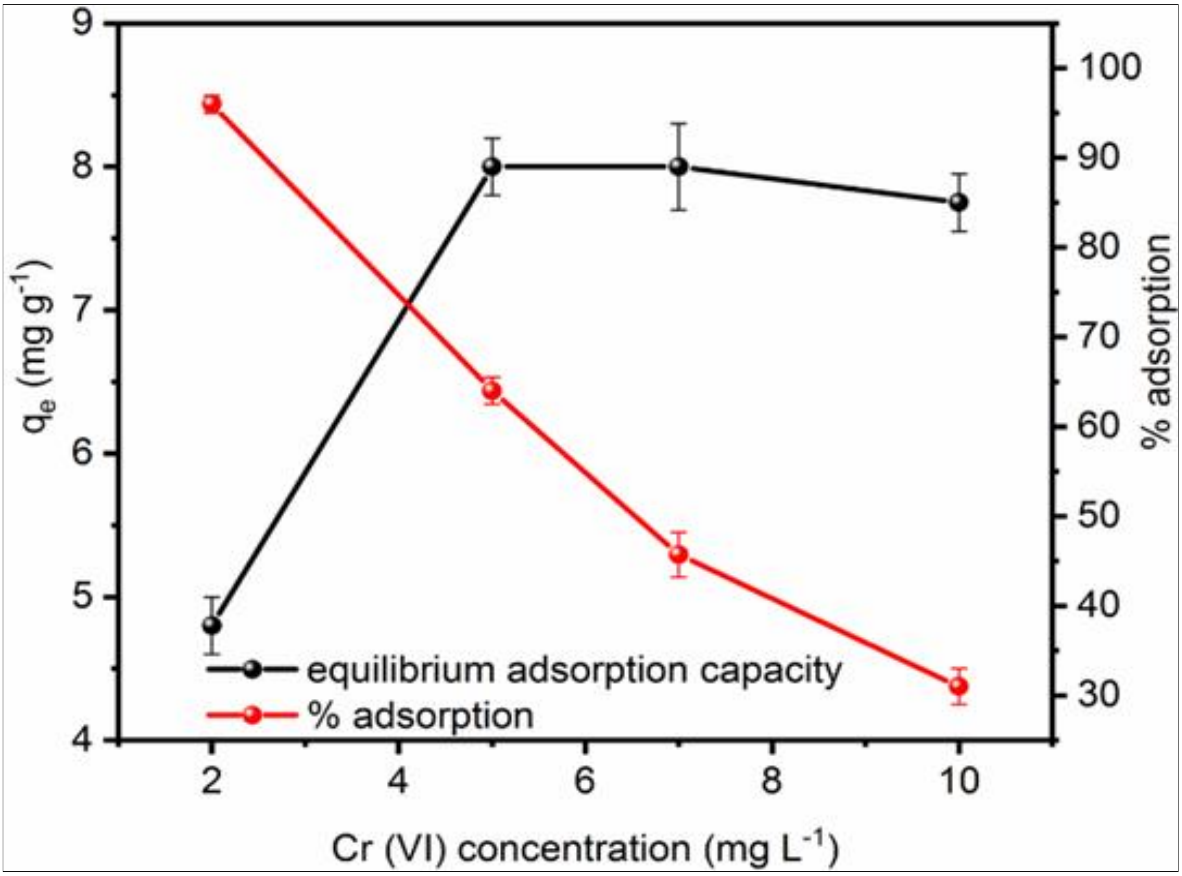

Fig 5: Percentage adsorption (red) & equilibrium adsorption capacity (black) of $FeSb_2$ for the removal of Cr(VI).

Table 1: Kinetic parameters for the removal of Cr(VI) onto FeSb2.

Kinetic models (25 °C, Natural pH and 0.4 g L^{-1} $FeSb_2$ dosage)						
Cr(VI) conc. (mg L^{-1})	**Pseudo-first-order**			**Pseudo-second-order**		
	K_1 (min^{-1})	q_e (mgg^{-1})	R^2	K_2 (g mg^{-1} min^{-1})	q_e (mg g^{-1})	R^2
2	0.028	4.746	0.911	0.0097	5.15	0.958
5	0.011	6.363	0.916	0.0103	6.55	0.991
7	0.013	5.483	0.875	0.0158	6.98	0.995
10	0.019	5.353	0.918	0.0145	7.47	0.992

Table 1: Isotherm parameters for the removal of Cr(VI) onto $FeSb_2$.

isotherm models (25 °C, natural pH and 0.4 g L^{-1} $FeSb_2$dosage)					
Langmuir isotherm			**Freundlich isotherm**		
q_m (mg g^{-1})	K_a (L mg^{-1})	R^2	K_F	n	R^2
7.79	17.82	0.999	6.712	8.37	0.84

Conclusion

We have presented a synthesis of FeSb2 particles via a simple co-precipitation approach using metal chlorides as precursors and their use for the removal of hexavalent chromium from aqueous solutions. The phase purity and morphological characteristics of the samples have been analyzed using XRD and SEM. The results revealed efficient removal of Cr(VI), even up to 96%. The present study should guide researchers to develop other intermetallics using transition-metal and main-group elements for other wastewater treatments.

Acknowledgement

Authors are thankful to institute instrumentation center (IIC), IIT Roorkee for providing sample characterization facilities.

References

1. Guo DM, An QD, Xiao ZY, Zhai SR, Shi Z. Polyethylenimine-functionalized cellulose aerogel beads for efficient dynamic removal of chromium (VI) from aqueous solution. RSC Adv, 2017:7:54039-54052.
2. Al Z, Cheng Y, Zhang L, Qiu J. Efficient removal of Cr(VI) from aqueous solution with Fe@Fe2O3 core-shell nanowires. Environ. Sci. Technol,2008:42:6955-6960.
3. Liu Q, Yang B, Zhang L, Huang R. Adsorptive removal of Cr(VI) from aqueous solutions by cross-linked chitosan/bentonite composite. Korean J. Chem. Eng,2015:3:1314-1322.
4. Anupam K, Dutta S, Bhattacharjee C, Datta S. Adsorptive removal of chromium (VI) from aqueous solution over powdered activated carbon: Optimisation through response surface methodology. Chem. Eng. J.,2011:173:35-143.
5. Bayuo J, Ba KBP, Abukari MA. Adsorptive removal of chromium(VI) from aqueous solution unto groundnut shell. Appl. Water Sci,2019:107:1-11.
6. Omer AM, Khalifa RE, Hu Z, Zhang H, Liu C, Ouyang XK. Fabrication of tetraethylenepentamine functionalized alginate beads for adsorptive removal of Cr(VI) from aqueous solutions. Int. J. Biol. Macromol,2019:125:1221-1231.
7. Mahmoud ME, Sharkawy RME, Ibrahim GAA. Promoted adsorptive removal of chromium(VI) ions from water by a green-synthesized hybrid magnetic nanocomposite (NFe3O4 Starch-Glu-NFe3O4ED). RSC Adv,2021:11:14829-14843.
8. Narayan R, Meena RP, Patel AK, Prajapati AK, Srivastava S, Mondal MK. Characterization and application of biomass gasifier waste material for adsorptive removal of Cr(VI) from aqueous solution. Environ. Prog. Sustain. Energy,2016:35:95-102.
9. Misra RK, Jain SK, Khatri PK. Iminodiacetic acid functionalized cation exchange resin for adsorptive removal of Cr(VI), Cd(VI), Ni(II) and Pb(II) from their aqueous solutions. J. Hazard. Mater,2011:185:1508-1512.
10. Huang G, Zhang H, Shi JX, Langrish TAG. Adsorption of chromium(VI) from aqueous solutions using cross-linked magnetic chitosan beads. Ind. Eng. Chem. Res,2009:48:2646-2651.
11. Bhattacharyya KG, Gupta SS. Adsorption of chromium (VI) from water by clays. Ind. Eng. Chem. Res,2006:45:7232-7240.
12. Yang C, Ju T, Wang X, Ji Y, Yang C, Lv H, *et al*. The preparation of a novel iron/manganese binary oxide for the efficient removal of hexavalent chromium [Cr(VI)] from aqueous solutions. RSC Adv,2020:10:10612-10623.
13. Gao H, Lv S, Dou J, Kong M, Dai D, Si C, *et al*. The efficient adsorption removal of Cr(VI) by using Fe3O4 nanoparticles hybridized with carbonaceous materials. RSC Adv. 00, 2015, 1-8.
14. Yu XZ, Zhang XH. Kinetics for adsorptive removal of chromium (VI) from aqueous solutions by ferri hydroxide/oxohydroxides. Ecotoxicology,2014:23:734-741.
15. Litefti K, Freire M S, Stitou M, Álvarez J G. Adsorption of an anionic dye (congo red) from aqueous solutions by pine bark. Sci. Rep,2019:9:16530.
16. Wong S, Ghafar NA, Ngadi N, Razmi FA, Inuwa IM, Mat R, *et al*. Effective removal of anionic textile dyes using adsorbent synthesized from coffee waste. Sci. Rep,2020:10:2928.
17. Li H, Li Q, He X, Zhang N, Xu Z, Wang Y, *et al*. The magnetic hybrid Cu(I)-MOF@Fe3O4 with hierarchically engineered micropores for highly efficient removal of Cr(VI) from aqueous solution. Cryst. Growth Des,2018:18:6248-6256.